Determination of porosity and storage capacity of a calcareous aquifer (France) by correlation and spectral analyses of time series

Stephane Bernard · Frederick Delay

Abstract Time-series analyses were used to investigate the relationships between barometric pressure changes, earth tides, and water-level fluctuations in a confined aquifer. The method was applied to data from the fractured aquifer at the Hydrogeological Experimental Site in Poitiers (France) and used to yield estimates of the aquifer's storage capacity, porosity and barometric efficiency. The aim is to address relevance of these analyses for an aquifer showing both fracture draining and confined karstic flow in thin strata. Cross-correlation and spectral analysis are used to compare water-level head and atmospheric-pressure fluctuations. Porosity and storage capacity are calculated using this method and compared to results from petrophysical measurements and hydraulic pumping tests, respectively. The storage coefficients calculated by the time-series analyses are in agreement with those obtained by interpretation of the interference pumping tests. Conversely, porosity values calculated by time-series analyses are underestimated compared to those obtained by other methods.

Keywords Hydraulic properties · Fractured rocks · Stress/strain (barometric tidal effects) · Time series · France

Introduction

Classical investigation techniques such as hydraulic pumping tests and tracer tests are essential for characterizing any type of aquifer. However, because of the limited investigation scale of these techniques, they do not always provide sufficient information on ground-water flow and its temporal variations. In addition, these tests cannot be improvised in the field because heavy equipment such as pumps, automatic samplers, head-probes, etc. are required. Preliminary studies are therefore useful to get a basic idea of how the aquifer behaves and then to delineate further work involving cumbersome and expensive experimental gear.

One of these preliminary approaches consists of using time-series analyses of barometric-pressure changes, earth tides, and water-level fluctuations (Box et al. 1994). Correlation and spectral analyses are based on a systemic approach that overlooks the physical fundaments of the problem and merely links, as in a black box, inputs to outputs. The aquifer is considered as a filter that keeps, eliminates or transforms input information (barometric-pressure changes and earth tides) to produce an output signal (water-level fluctuations). It is expected that the degree of transformation of the input signal will provide valuable information on the nature of the system (Larocque et al. 1998). Earth strains, even such small ones as those produced by earth tides, induce easily observable opposite-phased water-level fluctuations in wells. Analyses of water-level fluctuations caused by earth tides can be used to compute storage capacity and porosity of an aquifer. These parameters are of great interest to hydrologists for identifying flow and available groundwater resources. Water-level monitoring in wells drilled into confined aquifers is a basic tool to survey spatial and temporal changes of a system but it may also give information on dilatation of fluid-saturated rocks. It is known that water-level fluctuations in a well are controlled by tide, barometric, and tectonic effects. The components of tidal strain can be correlated with the water-level response and then studied by means of time-series analysis. The calculation of the aquifer storage capacity and porosity for the near vicinity of monitored wells is based on the analysis of water-level fluctuations as regards (Mangin 1984): (1) trend, periodicity and background noise; (2) auto-correlation in time (simple correlation and simple spectral analyses); and (3) cross-correlation in time (cross-correlation and cross-spectral analyses) with barometric pressure changes and earth tides. Usually, time-series analysis is performed over either karstic systems (e.g., Pinault et al. 2001) or continuous porous (and/or densely fractured) aquifers (Pinault et al. 2005).

In the present case, the method was applied to data from the Hydrogeologic Experimental Site (HES) in

Received: 14 February 2007 / Accepted: 10 May 2008
Published online: 19 June 2008

S. Bernard (✉) · F. Delay
UMR 6532, CNRS,
University of Poitiers,
Earth Sciences Building, 40 Avenue du Recteur Pineau,
86022, Poitiers, France
e-mail: stephane.bernard@ext.univ-poitiers.fr

 DOI 10.1007/s10040-008-0321-2

Poitiers, France. Ground water at HES exists in a fractured limestone aquifer which shows mixed flow between fracture matrix drainage and karstic features in confined thin layers (Bernard et al. 2006; Kaczmaryk and Delay 2007a). It is interesting to see whether or not time-series processing is hampered or biased by these mixed conditions merging localized flow at high velocity and classical diffusive drainage. To make it simple, water-level fluctuations in wells are directly correlated with external stress variations (barometric pressure, gravitational forces of earth tides). As suggested by Bredehoeft (1967), the amplitude of water-level fluctuations depends on the storage coefficient of the aquifer. When a continuous porous aquifer is compressed, the change in the total volume of a fluid-saturated porous medium due to the deformation of solid grains is small compared to the change in water volume. This assumption holds also for a widely open system such as a karstic network. In the end, a key assumption to the application of time-series analysis for hydraulic parameters identification is that nearly all the change in volume of the aquifer is that of the saturated zone. This assumption is apparently valid for granular porous media or open conduits in hard rocks, but it may not be valid for rocks such as a fractured limestone, even though it is riddled with pervasive conduits.

It must be noted that the limestone aquifer in Poitiers primarily behaves as a dual-porosity medium with classical slow draining, e.g., 2 m of head drawdown after 3 days of pumping at an observed well located 100 m away from a well pumped at 60 m^3 h^{-1} (Bernard et al. 2006; Kaczmaryk and Delay 2007a). However, the aquifer is almost evenly stressed whatever the distance from the pumped well because the pressure depletion propagates very rapidly through the open drains of the karstic layers. It has been shown recently that this very specific behavior could be mimicked by coupling a wave propagation (as in a so-called "sounding tube") to a dual-porosity medium approach (Kaczmaryk and Delay 2007b). It is obvious that this hydraulic behavior might bias the time-series analyses. This is one of the main reason motivating the present study, knowing that studies have not yet dealt with specific improvements of the methods prevailing in time-series analysis for groundwater flow. In this report, an estimation of the correlation of water level in wells with barometric pressure is given followed by a discussion of earth tides, an estimation of porosity and storage capacity of the aquifer, and finally a comparison of results to values determined by other methods.

Location and geologic setting

The site at which the time series has been recorded belongs to the University of Poitiers (France). The location of the experimental site is shown in Fig. 1. It has been designed for the purpose of providing facilities to develop research and engineering on subsurface flow and water resources management. The HES is located in west-central France (between (46°33′17″; 0°24′14″) and (46°33′28″; 0°24′26″) coordinates expressed in latitude and longitude, respectively) on the southern border of the Paris Basin. In this region, Jurassic limestone outcrops (or lays beneath a thin cover of Tertiary clays) and is slightly tilted toward the north. This monoclinic structure is cut by important sub-vertical faults from several tectonic phases between the Eocene and Pliocene epochs (Burbaud-Vergneaud 1987) with the development to the south of horst structures such as those of "Seuil du Poitou" and "Ligugé". To simplify, Jurassic aquifers are therefore sub-horizontal limestone vertically fractured along the N–S and E–W directions. To date, no reliable reference on the fracture density in the close vicinity of the site has been published. This is probably because outcrops are small and scarce in this area and only appear in conjunction with slightly elevated compartments of regional faults.

The site is located in one of the main regional aquifers, i.e., a mid-Jurassic (Dogger) limestone that is about 100 m thick. The limestone aquifer is confined beneath 10–25 m of Tertiary clays. The site encloses about 35 wells (fully penetrating open boreholes) spatially distributed as nested five-spots, i.e., a pattern with a well at the center and four wells at the corners of a square. Since 2002, measurements of water levels have been made by a digital-probe system (Datalogger MAC-10F, Paratronic, Reyrieux, France) with a resolution of 1 cm. All the wells are fitted with the same digital recording system, measuring water levels at 30-min intervals. The digital probe systems are isolated from meteorological effects (snow or rainfall). At the same time, a climatic station (Weather Monitor II, Davis Instr., Hayward, CA) located at HES recorded barometric pressure data at 30-min intervals with a 1.7 hPa (hecto-Pascal) resolution.

Methodology

Groundwater in all the wells located at HES fluctuate. As shown in Fig. 2, the water heads between July 2002 and April 2005 are perturbed by several drilling and pumping phases undertaken since early 2003. It must also be noted (Fig. 2) that the perturbations due to drilling and pumping operations mimic the general trend observed under temperate climates, i.e. a rapid increase of water level in winter due to net rainfall infiltration (where the aquifer is unconfined) followed by a gradual decrease in summer. This gradual decrease is slow here since the aquifer is confined and thus sheltered from high-frequency atmospheric variations. The decrease of water level during summer is mostly the consequence of an obvious increase of evapo-transpiration over the recharge areas and therefore a decrease of the mean inlet water fluxes. Despite the perturbations produced by the site construction, the seasonal variation of the piezometric head can be estimated at about 2.5 m between winter and summer. These fluctuations are in agreement with other values recorded from numerous points of observation distributed over a large surface area.

 DOI 10.1007/s10040-008-0321-2

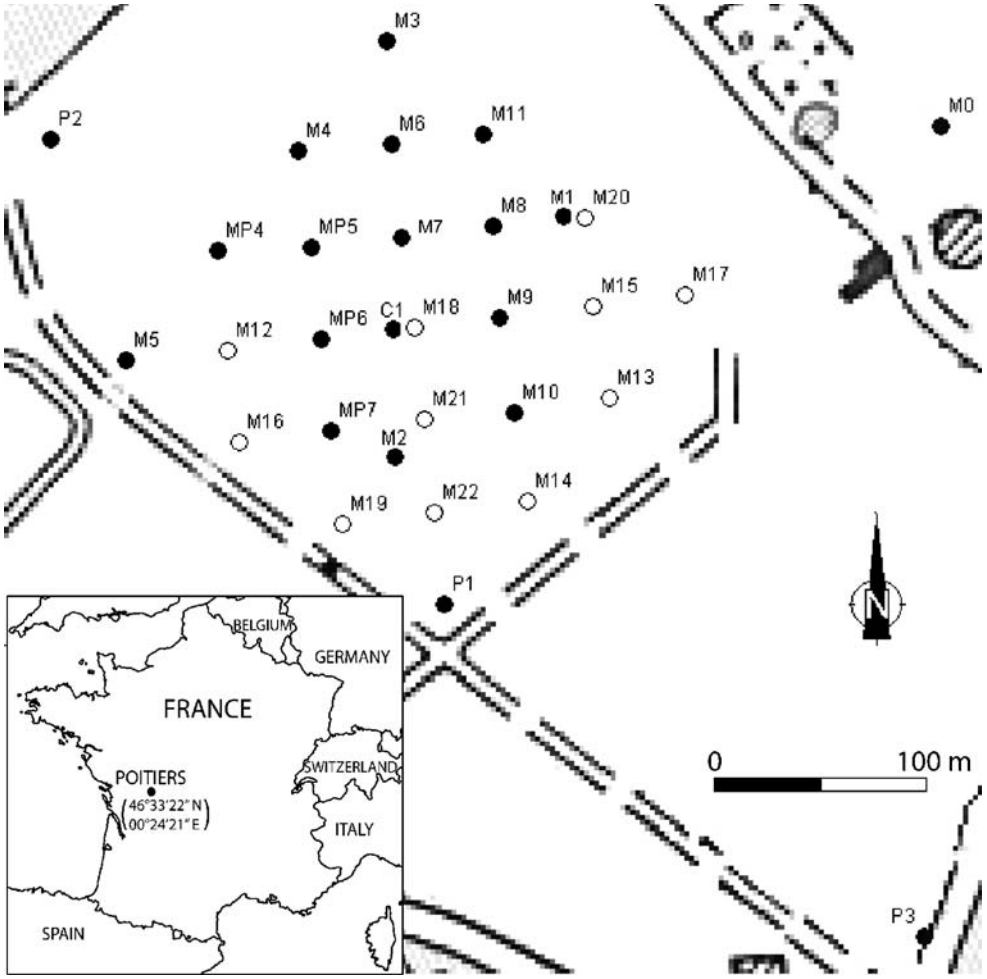

Fig. 1 Location of the Hydrogeological Experimental Site in France. *Solid and empty dots* correspond to wells drilled in 2004 and 2005, respectively

Spectral analysis reveals possible cycles and periodic components hidden in a time series. It is based on the Fourier Transform technique, which converts, in this case, a time series into a sum of periodic complex basis functions (also called harmonics), each characterized by a frequency and an amplitude. Correlation and spectral analyses are all the more significant and easy to perform as time-series are made of numerous weakly perturbed values. In that case, relationships between water levels and tidal effects on one hand and between water levels and barometric pressure on the other are visible and allow for the identification of the water-storage properties of the aquifer. As stated previously, periods of "natural" flow conditions at the HES have been limited due to drilling or pumping. Consequently, the series that can be used for correlation and spectral analyses are relatively short in time and include few data. In the present case, a window of 3 months of measures (at the 30-min time step) between April 2003 and July 2003 was kept as the reference set of head fluctuations for performing time-series analyses. This period follows the first campaign of drilling and pumping works held at the site. It shows a quite "normal" behavior of hydraulic heads without the huge fluctuations due to forced flow by pumping or oscillations due to air pressure injected by the down-hole pneumatic drilling hammer used to bore the wells (Fig. 2).

Barometric effects

The sampling of barometric pressure at the HES started in November 2002 and still goes on today. The plot in Fig. 3 shows a global constant behavior. Most of the variations appear random at first glance, with the barometric pressure ranging from 969.1 to 1,045.3 hPa and a mean value of 1,007.7 hPa. Comparisons between the data recorded by this station and those derived from a climatic station located at the Poitiers airport (15 km away) have been performed and show very few differences.

Mangin (1984) expressed the steady-state pressure condition at the impervious upper boundary of a confined aquifer by:

$$\Gamma + P_a = s + bP_w \tag{1}$$

with Γ (M L^{-1} T^{-2}) the geostatic stress of the overlying rock layers, P_a (M L^{-1} T^{-2}) the atmospheric pressure,

 DOI 10.1007/s10040-008-0321-2

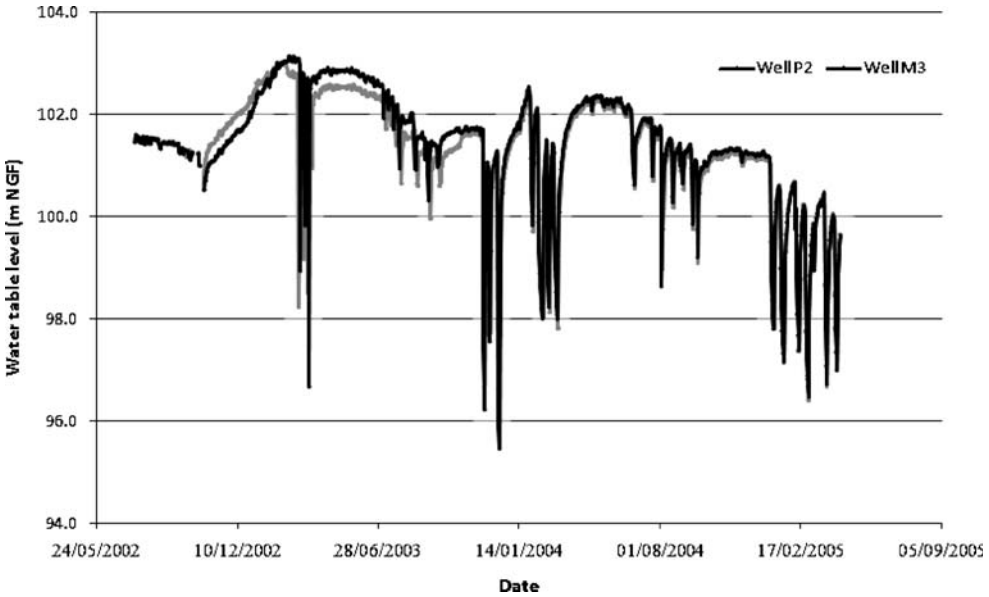

Fig. 2 Water level fluctuations in wells P2 and M3 from 17 July 2002 to April 2005

P_w (M L^{-1} T^{-2}) the pore fluid pressure, s (M L^{-1} T^{-2}) the effective vertical stress on the aquifer solid phase. The constant b, (dimensionless), corresponds to the contact surface ratio on which P_w is effective. The value of b depends on both the degree of consolidation of the rock and the nature of the contacts between grains. Assuming that for external stress variations, the compression of solid matter in the aquifer is insignificant as compared to change in porosity (see Introduction), b is equal to unity for an unconsolidated granular material and to porosity ϕ for a fully consolidated material. The steady-state hydraulic pressure head in the well is:

$$P_w = P_a + \rho g h \tag{2}$$

where ρ (M L^{-3}) is the fluid bulk density, g (L T^{-2}) the gravity acceleration, and h (L) the water head level as compared to a reference (generally the aquifer bottom). Jacob (1940) showed that an increase in the atmospheric pressure yields an increase in the compression stress and water pressure. Assuming that the geostatic stress Γ is constant, Eq. (1) can be written in terms of a change in barometric pressure as:

$$dP_a = ds + b dP_w \tag{3}$$

The notion of barometric efficiency (B) introduced by Jacob (1940) is defined as the ratio of the atmospheric pressure variation dP_a to the induced piezometric level variation dh. Parameter B (dimensionless), expresses the elastic response of the aquifer (material and pore water pressure) near the well. Thus, a hydrostatic fluctuation within the aquifer is equal to the atmospheric pressure variation minus the elastic response of the aquifer to this pressure variation.

$$dP_w = dP_a - B dP_a = (1 - B) dP_a \tag{4}$$

Therefore, identifying Eq. (4) to dP_w drawn from Eq. (2) allows the calculation of the water-level fluctuation in a well open over the whole aquifer thickness as:

$$dh = -B \frac{dP_a}{\rho g} \tag{5}$$

with dh being the water-level fluctuations due to the change dP_a in atmospheric pressure (Fitts 2002).

Barometric pressure time series shows both random and structured features and can be considered as regionalized variables (Matheron 1965), with the restriction that the spatial reference is the time axis and not the classical Euclidean space. A fast Fourier transform to look for periodicity was applied, but any trend that may exist in the time series was first removed using a first differencing:

$$D_t^{\chi} = Y_t - Y_{t-\chi} \tag{6}$$

This is a classical technique widely used in Geostatistics to get stationary quantities when the variable itself (Y) is obviously subjected to non-constant trends over space (or time). If the first difference is efficient then $E\ [Y_t - Y_{t-1}] = 0$ with E[] the mathematical expectation operator. Thus, the time series D_t^1 has a stationary mean (e.g., no trend in mean value). The calculation of its autocorrelation function (see the following for details of calculation) shows a rapid decrease with the time-lag and then slight oscillations around zero (Fig. 3b). This means that the barometric pressure is a stationary process at low frequencies (i.e., over large time periods), with a rapid decrease of correlation between signals sampled with increasing time-lags. Note that the correlation function is calculated here with the same elementary time step (30-min) as that of raw barometric data and this

 DOI 10.1007/s10040-008-0321-2

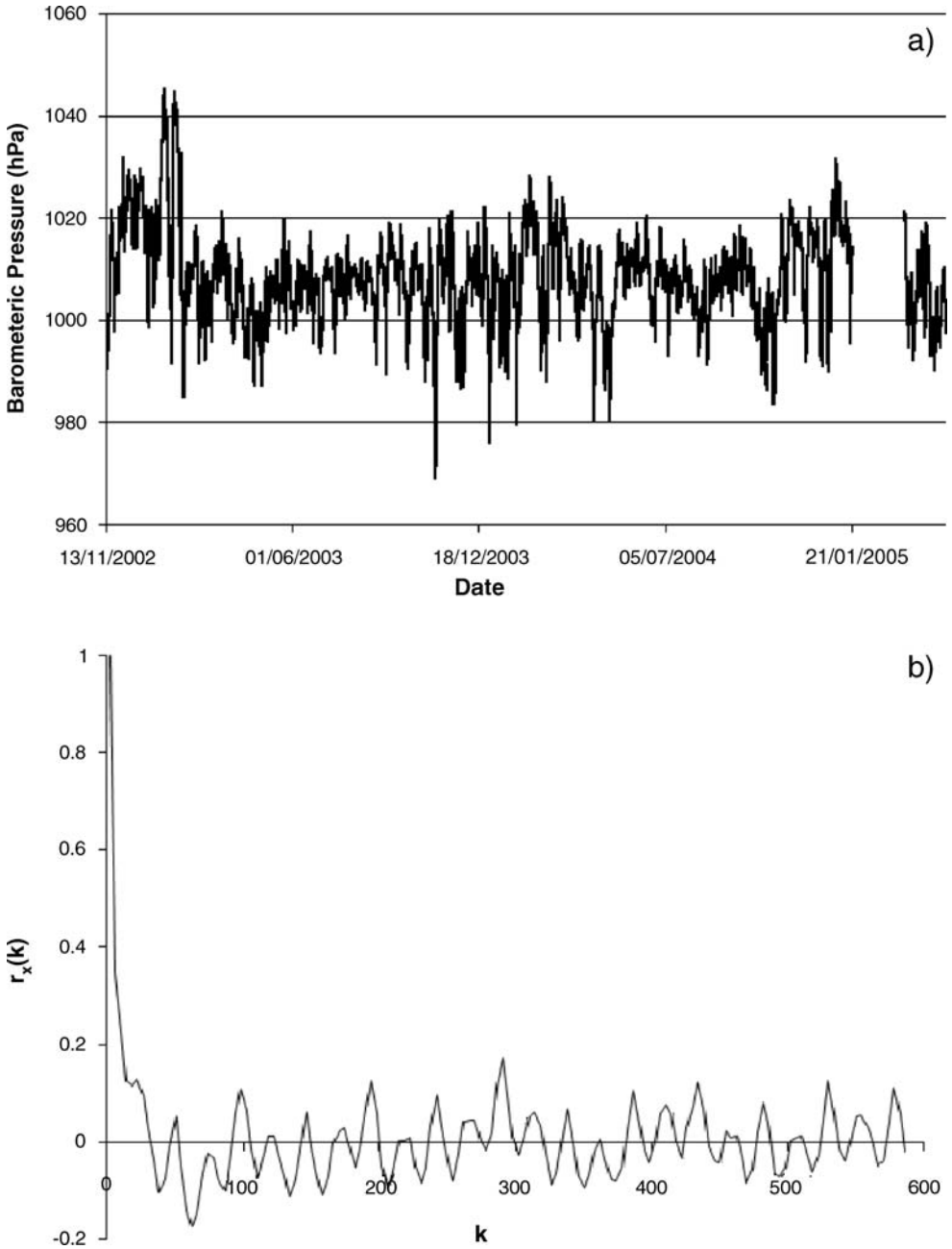

Fig. 3 **a** Barometric pressure recorded by the climatic station in the experimental site at a 30-min frequency. **b** Autocorrelation function, rx(k), after first-order differencing. Autocorrelation is calculated with an elementary time step of 30 min and the time axis on the plot is labeled in numbers of time steps (k)

function is about zero beyond 20 h (i.e., k number of time steps=40 in Fig. 3b). It should be mentioned that in theory it exists as a semi-diurnal barometric tide but the fluctuation range is too small to be recorded by the well equipment. The barometric tide is therefore neglected as compared to the effect of the earth tide.

Tidal effects

Tidal effects cause an elastic-viscous deformation of the Earth and are created by the gravitational attraction of the Moon, the Sun and, to some extent, of other planets. The degree of fluctuation of heads in the well-aquifer association depends on the well size, the aquifer characteristics (porosity and storage capacity) but also on the period and amplitude of the perturbing wave (Bredehoeft 1967; Melchior 1978). In theory, the number of tidal waves composing the earth tide spectrum is infinite, but only large amplitudes have some influence on the aquifer and only five waves (labeled M2, S2, N2, K1 and O1) are responsible for 95% of the water-level fluctuations observed in a well (Box et al. 1994). These waves are regrouped into two types: tesseral waves with a diurnal period (approximately 24 h) and sectorial waves of semi-

 DOI 10.1007/s10040-008-0321-2

diurnal period (approximately 12 h). The Tsoft software developed in the Royal Observatory of Belgium (Van Camp and Vauterin 2005) has been used to compute the theoretical earth tide at the HES location, accounting for both latitude–longitude coordinates and elevation (Fig. 4). The earth tide will be used later to find waves able to influence water levels.

Correlation and spectral analysis method

The expressions used to obtain the coefficients (which will be developed in the following) for correlation and cross-spectral analysis functions follow the work by Jenkins and Watts (1968). Let us take two discretized chronological series: the first one is the input denoted x_t (x_1, x_2, ..., x_n) of the aquifer (i.e. system), and represents barometric pressure or gravitation fluctuations. The observed response are water-level fluctuations y_t (y_1, y_2, ..., y_n), n is the total number of data pairs available. The simple-correlation analysis quantifies the linear dependency of successive values in a single time series and addresses this dependency as a function of the time lag between values. The cross-correlation analysis proceeds in the same way except that correlation is calculated between two time series, e.g., the input x_t and the output y_t. The cross-correlation function provides information on the causal and non-causal relationships between the input and the output and helps to constrain system parameters, in this case storage and porosity (Larocque et al. 1998).

The cross-correlation function $r_{xy}(k)$ can be written as:

$$r_{xy}(k) = \frac{C_{xy}(k)}{\sigma_x \sigma_y}; \quad C_{xy}(k) = \frac{1}{n-k} \sum_{t=1}^{n-k} (x_t - \overline{x})(y_{t+k} - \overline{y}) \tag{7}$$

where $C_{xy}(k)$ is the cross-correlogram, σ_x and σ_y are the standard deviations of the time series, k is the time lag (k=0 to m with m<<n), $\overline{x}$ and $\overline{y}$ are the mean of each time series and m is the cutting threshold defining the maximum time lag over which the correlation is calculated. This cutting threshold is usually chosen to grasp a given behavior at prescribed lags: daily, weekly, monthly or annual. Note that the cross-correlogram in Eq. (7) is not symmetric. Note also that the auto-correlation function obeys the same equations as Eq. (7) with y=x and is symmetric.

The spectral analysis is complementary to the correlation analysis. The spectral density function corresponds to a change from a time mode to a frequency mode through a discrete Fourier transform of the auto-or cross-correlation function. For an auto-correlation function, the spectral density function can be written as:

$$S(f) = 2\left[1 + 2\sum_{k=1}^{m} D(k) r_{xx}(k) \cos(2\pi f k)\right] \tag{8}$$

where f=j/2m and j=1 to m, f is the frequency, $r_{xx}(k)$ is the auto-correlation function (in the real space) and $D(k)$ is a weighting function that defines the amplitudes of the harmonics [$r_{xx}(k)$cos(2πfk)] of $S(f)$. Among the numerous weighting functions available, the one found to be most suited to the interpretation of hydrological data is given by (Jenkins and Watts 1968; Mangin 1984):

$$D(k) = \frac{1}{2}\left(1 + \cos\pi\frac{k}{m}\right) \tag{9}$$

The cross-spectral density function, $S_{xy}(f)$, is expressed as a function of the co-spectrum, $h_{xy}(f)$ and the quadrature

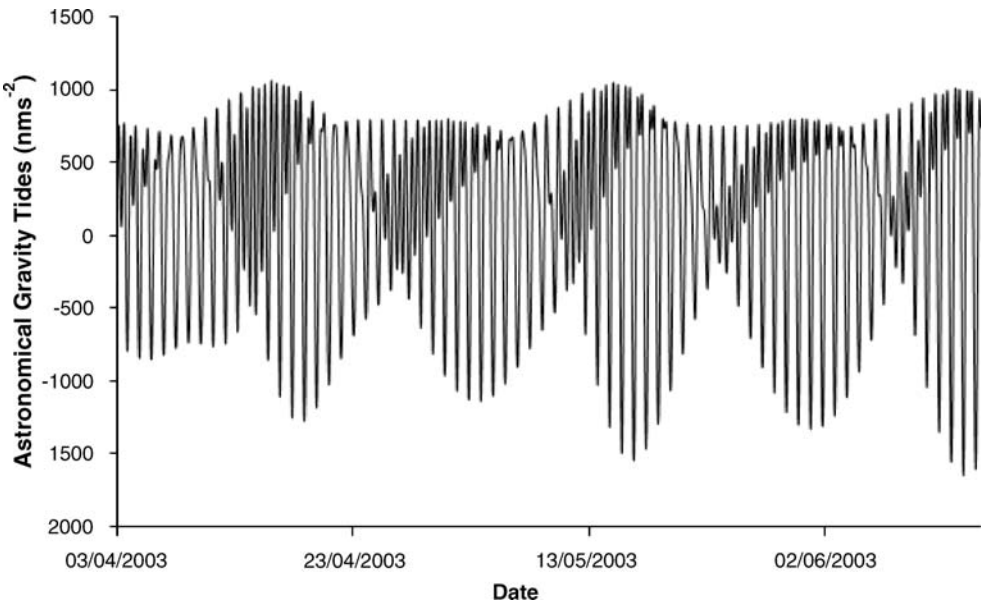

Fig. 4 Theoretical earth tide at the Hydrogeological Experimental Site computed by the Tsoft software (Van Camp and Vauterin 2005)

 DOI 10.1007/s10040-008-0321-2

spectrum, $\lambda_{xy}(f)$, i.e., the classical real and imaginary part of a discrete Fourier transform written as:

$$S_{xy}(f) = h_{xy}(f) - i\lambda_{xy}(f)$$
$$h_{xy}(f) = 2\left[r_{xy}(0) + \sum_{k=1}^{m}\left(r_{xy}(k) + r_{xy}(k)D(k)\cos(2\pi f k)\right)\right]$$
$$\lambda_{xy}(f) = 2\left[r_{xy}(0) + \sum_{k=1}^{m}\left(r_{xy}(k) + r_{xy}(k)D(k)\sin(2\pi f k)\right)\right] \quad (10)$$

The amplitude function drawn from (Eq. 10) identifies the way in which the magnitude of the input signal has been modified by the system and is simply written as the square root of the second-order norm of S_{xy}: $|S_{xy}(f)| = \sqrt{h_{xy}^2(f) + \lambda_{xy}^2(f)}$

Other functions can be defined on the basis of the spectral and cross-spectral density functions, in particular the gain can be expressed as—e.g., Padilla and Pulido-Bosch (1995):

$$G_{xy}(f) = \frac{S_{xy}(f)}{\sqrt{S_x(f)}} \quad (11)$$

The gain function expresses the amplification or attenuation of the input data, attributable to the system and it may be of great interest in the context of the present study. When derived from cross-analyses between barometric pressure (input signal x) and water level (output signal y) the gain can be equated to the barometric efficiency defined by Jacob (1940; see Eq. (5)). Recall that the barometric efficiency expresses the elastic water-level response as a consequence of the stress exerted on the confined aquifer by the atmospheric pressure. With the definition Eq. (11) given above and for time lags of 12 or 24 h, the barometric efficiency measures how much the head level amplifies or dampens barometric fluctuations after 12 and 24 h.

As briefly discussed already (see Introduction), it is assumed that nearly all the change in the volume of the aquifer is that of the saturated zone. Thus, the combination of the barometric pressure effect and the earth tide influence allows for the evaluation of the porosity and storage coefficient of the confined aquifer by solving two straightforward equations. This yields a handy tool, simpler and less expensive than a hydraulic pumping test. The determination is performed for one observation point irrespective of the aquifer transmissivity and the method is the sole alternative to evaluate storage capacity at the well scale except the "push–pull" tracer test in a single well. Push-Pull tracer tests are based on the injection at a rate q of a mass of tracer and then its withdraw at the same rate q. Basically, this method is aimed at screening all reversible transport mechanisms due to fluid flow and then exhibits non-reversible features. For instance, advection + mechanic dispersion are overlooked and the results show only the effects of retention mechanisms (e.g., matrix diffusion). Incidentally, storage capacity can be drawn from the interpretation of the test since it conditions the mean resting time of the tracer in the vicinity of the well. However, interpretation of the push–pull experiments remains complex (see e.g., Becker and Shapiro 2003).

Barometric efficiency B is obtained by cross-analyses (Eq. 11) between barometric pressure (input signal) and head levels (output signal). The observation of barometric effects informs on the volume porosity ϕ of the aquifer in the vicinity of the well, a quantity that is difficult to assess in hydrogeology. Its value is given by (e.g., Arditty 1978; Merritt 2004):

$$\phi = \frac{(\Theta E_w)}{(dh\rho g) + (1 - B)\Theta E_w} \quad (12)$$

where Θ (dimensionless) is the theoretical aquifer dilatation generated by the M2 tidal wave, and dh is the head variation amplitude. The calculated value of Θ, determined by the PREDICT software (from Wenzel's ETERNA package, available free online; Wenzel (1995)) equals 8.86×10^{-9} nstrain, strains are determined within a factor of 2 only (B. Ducarme, ICET Royal Observatory of Belgium, personal communication, 2006). E_w (M L^{-1} T^{-2}) is the elasticity module of water equal to 2.05×10^{6} kPa.

Jacob (1940) proposes to formulate the storage coefficient as a released volume of water derived from the fluid decompression and the solid part arrangement. This can be expressed as:

$$S = \frac{\rho g e}{E_w\left[\frac{1}{\phi} + (B - 1)\right]} \quad (13)$$

with e (L) being the aquifer thickness (here=100 m) and ϕ the porosity determined from barometric effects by Eq. (12).

Application to data from HES and discussion

The methodology depicted above is used on data from the HES to identify porosity and storage capacity in the vicinity of the wells. The very rapid decrease shown by the auto-correlation function of the barometric pressure time series (Fig. 3b for the correlation function, Fig. 5 for its spectral density), calculated after first-order differencing, is symptomatic of a phenomenon with a weak temporal correlation. This is one of the assumption required to apply time-series analyses (e.g., Larocque et al. 1998).

In contrast, the auto-correlation function of the earth-tide time series calculated from Eq. (7) has obviously a well-defined periodic structure. These results are confirmed by the spectral density analysis. Figure 6 shows that the four most important peaks of the spectral function from earth tides correspond to the five major tidal waves: O1 with period of 1.07 day, K1 at 0.99 day, M2 and N2 merged together in the peak at 0.52 day and finally the S2 wave at 0.5 day (Melchior 1978). Since Eqs. (11)–(13)

 DOI 10.1007/s10040-008-0321-2

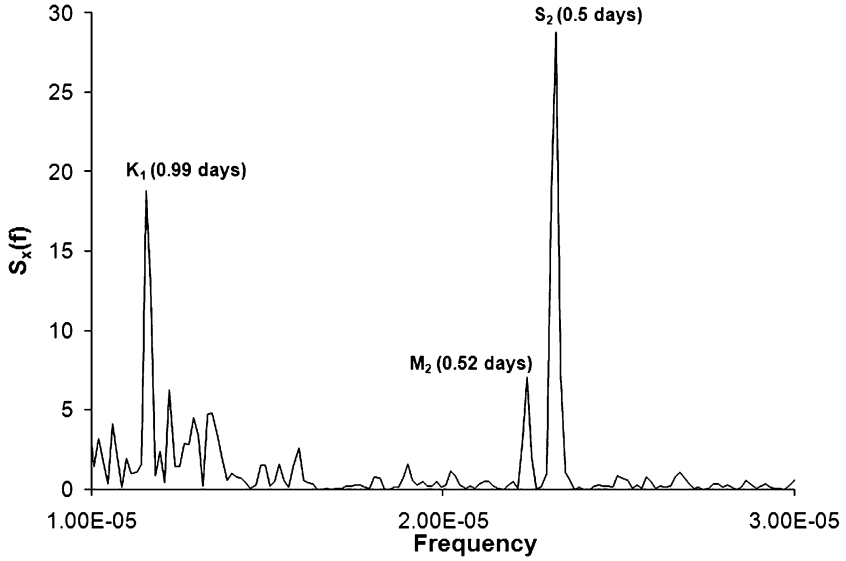

Fig. 5 Barometric pressure time series: spectral density function

refer to a specific frequency f to calculate the barometric efficiency and the aquifer dilatation, this frequency should be the highest-one with the largest amplitude (in the hope it has significant effects on water levels). To choose the largest frequency allows potentially for identifying effects with lower frequencies. In the present case, it seems that the M2–N2 (at 0.52 day) wave of the earth-tide spectrum is well suited. It must be checked however that this wave is also visible on the water-level spectrum.

The auto-correlation and spectral density functions of water levels recorded in time at several HES wells have been calculated (an example is given in Fig. 7). The auto-correlation function (not reported here) slowly decreases with time lag between data and expresses a well-correlated and structured phenomenon. Again, this is a prerequisite to the time-series analyses. The spectral density of water levels shows two main periodic components of the signal displayed at 0.52 and 0.5 day frequency. The most important peak (S2), which is also visible in Fig. 3b, can be considered as a pollution effect inferred by the atmospheric pressure. Thus, the maximal amplitude of the head-level fluctuations is due to the referenced wave M2 as illustrated in Fig. 6 (period: 12 h 25 min 14 s). Similar results were also obtained for all other monitored wells of the HES. In the following, the periodic cubic dilatation induced by the tidal M2 wave was used as reference for the frequency f in $S_x(f)$ and $S_{xy}(f)$ for the determination of the porosity and storage capacity.

Table 1 summarizes storage capacity and porosity values resulting from the above analysis applied to seven wells of the HES. The estimated parameters are not significantly different between the seven wells tested with values ranging from 1.12 to 2.36% for porosity and from 1.71×10^{-5} to 5.80×10^{-6} for the storage capacity. These

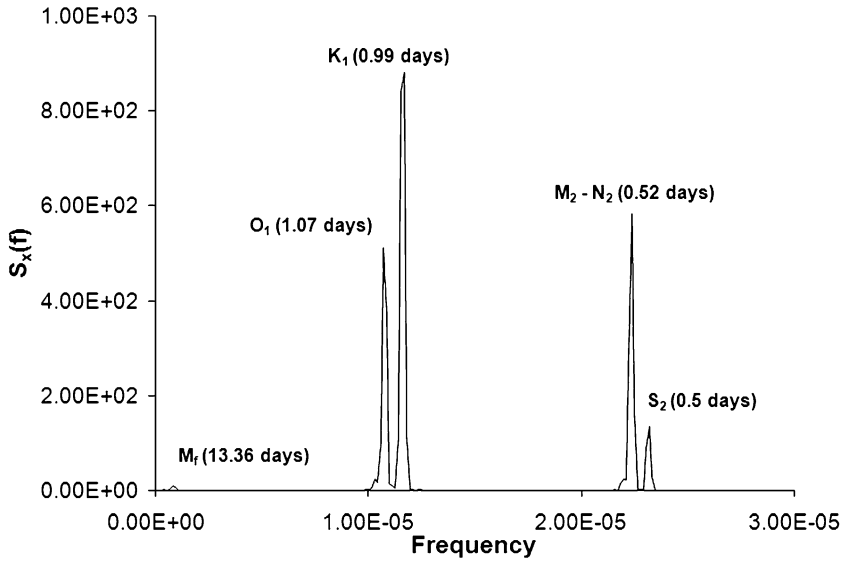

Fig. 6 Earth tide time series: spectral density function

 DOI 10.1007/s10040-008-0321-2

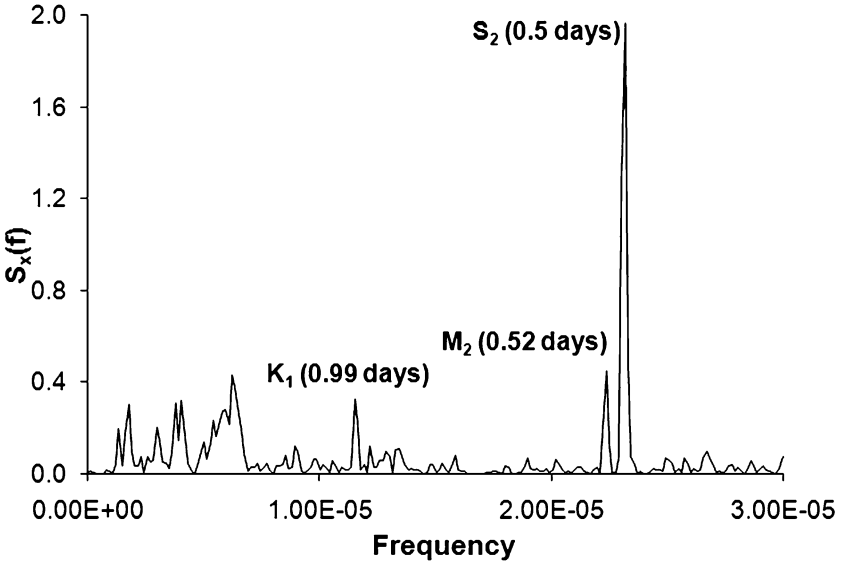

Fig. 7 Water level time series: spectral density function

values of porosity and storage capacity are perfectly compatible with values encountered in other similar aquifers and lie in ranges for which the correlation and spectral analyses can be applied. Mangin (1984) has shown that the observation of the tidal effect is only possible in a confined aquifer with a storage capacity in the order of or less than 10^{-5}.

In order to check the relevance of the porosity and storage capacity values obtained from correlation and spectral analyses, the results were compared with those from two other methods: (1) petrophysical measurements from drill cuttings, which give an evaluation of the porosity at the direct vicinity of the well drilled, and (2) models for interpreting interference pumping tests, which give the storage capacity over a larger area than the close vicinity of the well.

Porosity measurements from cuttings are based on a pressure pulse applied to a cell filled with cuttings saturated by a viscous fluid and a trapped gas initially at atmospheric pressure. The porosity is derived from the transient response of the oil invasion into the cuttings by using a numerical model (Egermann et al. 2002; Egermann 2004). The limitations of the method are mainly related to the size and the representativeness of the drill cuttings. This method was applied to drill cuttings from well M7 and to fragments of a core sample from well C1. Porosity values varying in the range 10–20% for well C1 (mean equal to 14.77%) and in the range 10–15% for well M7 (mean equal to 12.32%) are obtained using this method. The porosity values measured from drill cuttings are greater than those evaluated by the correlation and spectral analyses (1.5–2% on average, see Table 1).

Porosity values may differ from time series to drill-cuttings simply because the scale experienced by both methods is different. As stated above, porosity of cuttings is important, say 15% on average, but the permeability of the cuttings (i.e., the limestone material without fractures, open conduits, joints between strata, etc.) is very small, 10^{-17} m^2 (unpublished results), i.e. about 10^{-10} m s^{-1} for the hydraulic conductivity. It is obvious that the porous matrix at the local scale is not very conductive and probably not well sampled by flow and pressure variations at the macroscopic scale (because of the weak connectivity of the pore space). On the other hand, it can be questioned on the scale over which a time-series interpretation for determining porosity is relevant. Barometric changes and Earth-tides forcing obviously act at a very large scale, and it can be envisioned that head fluctuations may represent the aquifer's response at a wide scale. However the problem is probably more tricky. A uniform stress applied over a wide portion of the aquifer does not necessarily imply that time-series analyses yield hydraulic parameters aggregated at the scale of the external constraints. Wells show different answers that could be interpreted as the "local" answer to a uniform large-scale external constraint. Then the question is, How to clearly define the scale over which the response at a well is relevant? On one hand this response convolutes in space the local influences of a wide uniform external forcing. This should yield quite similar local responses whatever the observed well. On the other hand, since responses at

Table 1 Storage capacity and porosity calculated from head fluctuations at different wells of the site (location in Fig. 1)

Well	Barometric efficiency	Δh (m)	Storage capacity	Porosity (%)
M1	0.591	0.09	$1.65\times\times10^{-5}$	2.1
M2	0.643	0.08	1.71×10^{-5}	2.4
M3	0.899	0.17	5.80×10^{-6}	1.1
M4	0.799	0.13	8.51×10^{-6}	1.5
M5	0.788	0.11	1.02×10^{-5}	1.7
P2	0.946	0.12	8.07×10^{-6}	1.6
P3	0.545	0.11	1.47×10^{-5}	1.7

Barometric efficiency is calculated according to Eq. (11) and Δh is the amplitude of head fluctuations used to calculate porosity from Eq. (12)

 DOI 10.1007/s10040-008-0321-2

each well may differ, this raises the question of the influence of the local context on the convolution of the inlet signal over a wider area. Note that observing lower porosity values from time series may be consistent with values averaged over wide areas in fractured rocks. For instance, with the fractal assumption used among other representations of the medium to interpret interference testing (see the following), the porosity slowly decreases with the distance experienced by the test.

In any case, the local vs. large-scale support of measures could explain the gap between values of porosity from percolation in the drill cuttings and from time-series interpretations. However, it must be noted that karstic flow in thin layers crossed by the wells may hinder time-series interpretations. Vertical flow along wells and transverse "leaks" may perturb both the static water-level pressure and the transmission of external stresses. Finally, each well can be viewed as the body of a flute with pressure of fluids inside the tube influenced by the number of closed or open vents. Of course, this is an image, but it may figure, in a simplified manner, the geometric settings of a well passing through layers enclosing open conduits. Given the form in Eq. (12), the effects of localized flow may influence either the barometric efficiency or the aquifer dilatation. This point will be addressed after discussing results on storage capacity.

Hydraulic interference tests have been widely used in hydrogeology and petroleum engineering to assess the hydraulic parameters of underground reservoirs. Delay et al. (2004) have proposed a new logarithmic approximation to the solution for interference pumping tests in a radial flow. It can be viewed as a generalization to fractured fractal media of the two-dimensional Jacob analytical solution by the introduction of scaling laws for permeability and storage coefficient. The analytical method and its inversion have been applied to a series of interference pumping tests carried out over the HES. Storage capacity values determined by this method range between 1×10^{-3} and 5×10^{-5}, but decrease with distance much more rapidly than expected from scaling power-law of fractal media. Another attempt was carried out by means of dual-porosity-media approaches (Kaczmaryk and Delay 2007a, b). On average, storage capacity for the fracture medium is in the range 10^{-5}–10^{-4} and storage capacity of the matrix medium in the range 10^{-4}–10^{-3}. Correlation and spectral analyses yield storage capacity values between 1.71×10^{-5} and 5.80×10^{-5}. These values from correlation and spectral analyses are of the same order as the lowest values from the fractal interpretation of interference pumping tests or of the same order as the fracture storage capacity of the dual-porosity-medium approach.

In a porous fractured medium, it is well known that at the large scale—including matrix, fractures, open joints between strata, etc.—the storage capacity is controlled by a macroscopic compressibility. The latter is a composite value between fluid compressibility, solid compressibility and ability of fractures and other open features to warp under pressure. The composite value is often one order of magnitude larger than the fluid compressibility—$1/E_w$ in Eq. (13)—used to determine the storage capacity from time series (Audouin et al. 2008). This may explain why time-series analyses tend to give the smallest values obtained by interference tests. Finally, times series would yield values more influenced by the fluid compressibility than by the composite value of the medium. This is consistent with the fracture storage capacity of a dual medium and also with the general state of the limestone around a well. The close vicinity of the well is deeply influenced by the damaged zone due to drillings (Audouin et al. 2008) and also in the present case, by the intersection with thin karstic layers. Open drains riddling these thin layers represent near the well an open volume ratio larger than away from the well (on average, the volume of the drains evolves with the distance r from the well, whereas the total cylindrical volume around the well evolves in r^2). All these features are consistent with a storage capacity near the well more influenced by the fluid compressibility (the storage capacity is therefore smaller) than by the macroscopic compressibility at the large scale. This small storage capacity is that viewed by time-series analyses.

Referring to Eq. (13), it can be noted that porosity takes part in the storage coefficient calculation. In order to evaluate the importance of porosity in the storage coefficient calculation, storage coefficients were calculated for different porosity values. The latter are given equal to those obtained by time-series analysis (1.1–2.4%) and by measurements on drill cuttings (10–20%), respectively. The results reported in Table 2 show a fair sensitivity of storage capacity to changing porosity values. More exactly, multiplying the porosity by a factor ten increases the storage capacity of about one half order of magnitude. This is of course not negligible but relatively weak compared with statistical variations of local values encountered in fractured porous media (e.g., Huang et al. 2004).

Finally, it seems that the barometric efficiency calculated from the time series (barometric pressure as input, water level as output) is relevant since it gives good results for the calculation of the storage capacity. This would mean that failure in calculating porosity is the consequence of an underestimation of the aquifer dilatation generated by the M2 tidal wave (see preceding). As stated above about compressibility including several features (fluid, rock matrix, open joints, fractures, etc.), it is probable that the non-homogeneity of the aquifer around the well, i.e., a fractured damaged zone, inter-

Table 2 Comparison between storage capacities calculated for different porosity values

Well	ACS porosity (1.1–2.4%)	Drill cuttings porosity (10–20%)
M1	1.65×10^{-5}	8.02×10^{-5}
M2	1.71×10^{-5}	8.30×10^{-5}
M3	5.80×10^{-6}	2.90×10^{-5}
M4	8.51×10^{-6}	4.22×10^{-5}
M5	1.02×10^{-5}	5.04×10^{-5}
P2	8.07×10^{-6}	4.04×10^{-5}
P3	1.47×10^{-5}	7.14×10^{-5}

 DOI 10.1007/s10040-008-0321-2

sections with open conduits, induces an increased dilatation compared to the theoretical one.

Conclusions

Characterizing the hydrodynamics of a confined aquifer requires determining hydraulic parameters such as permeability, storage coefficient and porosity. This report presents time-series analyses used to investigate the relationships between barometric pressure changes, earth tides, and water-level fluctuations measured in a fractured confined aquifer at the Hydrogeological Experimental Site in Poitiers (France). Flow is complex because of the mixing of classical diffusive drainage and karstic flow localized in thin layers riddled with open conduits.

Results presented in this report indicate that time-series analyses can be considered to be accurate for determining storage coefficient and they yield values comparable to that obtained by interpretation of interference pumping tests. In contrast, the porosity values calculated with time series seems to be greatly underestimated compared to the values obtained from drill cutting analyses. It is likely that the water pressure signal in the aquifer as well as external stress transmissions are slightly biased by mixed flow. The latter is partly the consequence of localized open conduits in thin layers which generate vertical motion of water in the wells passing through these layers.

Porosity, which is calculated directly from water-level variations and barometric efficiency, is hampered by "leaks" along the well. On the other hand, the storage coefficient value is calculated from the porosity derived from time-series analysis. However, a rapid calculation shows that the storage coefficient is not very sensitive to porosity variations. So even if the calculated porosity values are not representative of the natural medium, storage coefficients drawn from time series can be considered as accurate and representative of the medium at the immediate vicinity of the tested well. This makes these analyses still useful even for complex flow mixing classical diffusive drainage and karstic features.

Acknowledgements The authors are grateful to the French National Research Program in Hydrology and the "Poitou-Charentes" Water Research Program which partly funded this work. The authors thank Bernard Ducarme for his scientific support and helpful comments.

References

Audouin O, Bodin J, Porel G, Bourbiaux B (2008) Flow-path structure in a limestone aquifer: Multi-borehole logging investigations at the hydrogeological experimental site of Poitiers (France). Hydrogeol J. DOI 10.1007/s10040-008-0275-4

Arditty PC (1978) The earth tide's effects on petroleum reservoir. PhD Thesis, Standford University, USA, 140 pp

Becker MW, Shapiro AM (2003) Interpreting tracer breakthrough tailing from different forced-gradient tracer experiment configurations in fractured bedrocks. Water Resour Res 39(1):1024. DOI 10.1029/2001WR001190

Bernard S, Delay F, Porel G (2006) A new method of data inversion for the identification of fractal characteristics and homogenization scale from hydraulic pumping tests in fractured rocks. J Hydrol 328:647–658. DOI 10.1016/j.jhydrol.2006.01.008

Box GEP, Jenkins GM, Reinsel GC (1994) Time series analysis: forecasting and control, 3rd edn. Prentice Hall, Englewood Cliffs, NJ

Bredehoeft JD (1967) Response of well-aquifer systems to earth tides. J Geophys Res 72:3075–3087

Burbaud-Vergneaud M (1987) Fracturation et interactions socle-couverture: le Seuil du Poitou [Fractures and bedrock sedimentary cover interactions: Seuil du Poitou]. PhD Thesis, University of Poitiers, France

Delay F, Porel G, Bernard S (2004) Analytical 2D model to invert hydraulic pumping tests in fractured rocks with fractal behavior. Geophys Res Lett 31(16), DOI 10.1029/2004GL020500

Egermann P (2004) Petrophysical measurements from drill cuttings: an added value for the reservoir characterization process. Soc. Petrol. Eng. 88684, ATCE, San Antonio, TX, USA

Egermann P, Lenormand R, Longeron D, Zarcone C (2002) A fast and direct method of permeability measurements on drill cuttings. Soc. Petrol. Eng. 77563, ATCE, San Antonio, TX, USA

Fitts CR (2002) Groundwater science. Academic, San Diego, CA, 450 pp

Huang W, Di Donato G, Blunt MJ (2004) Comparison of streamline-based and grid-based dual porosity simulations. Soc Petrol Eng J 43(2):129–137

Jacob CE (1940) On the flow of water in an artesian aquifer. Trans Am Geophys Union 2:574–786

Jenkins GM, Watts DG (1968) Spectral analysis and its applications. Holden, San Francisco, 525 pp

Kaczmaryk A, Delay F (2007a) Interpretation of interference pumping test in fractured limestone by means of dual-medium approaches. J Hydrol 337:133–146. DOI 10.1016/j.jhydrol.2007.01.004

Kaczmaryk A, Delay F (2007b) Improving dual-porosity-medium approaches to account for karstic flow in a fractured limestone: application to the automatic inversion of hydraulic interference tests. J Hydrol 347(3–4):391–403. DOI 10.1016/j.jhydrol.2007.09.037

Larocque M, Mangin A, Razack M, Banton O (1998) Contribution of correlation and spectral analyses to the regional study of a large karst aquifer (Charentes, France). J Hydrol 205:217–231

Mangin A (1984) Pour une meilleure connaissance des systèmes hydrologiques à partir des analyses corrélatoire et spectrale [Toward a better knowledge of hydrologic systems by the use of correlation and spectral analyses]. J Hydrol 67:25–43

Matheron G (1965) Les variables régionalisées et leur estimation [Regionalized variables and their estimation]. Masson, Paris, 185 pp

Melchior P (1978) The tides of the planet Earth. Pergamon, Paris, 609 pp

Merritt ML (2004) Estimating hydraulic properties of the floridan aquifer system by analysis of earth-tide, ocean-tide and barometric effects: Collier and Hendry counties Florida. US Geol Surv Water Resour Invest Rep 03-4267, 70 pp

Padilla A, Pulido-Bosch A (1995) Study of hydrographs of karstic aquifers by means of correlation and cross-spectral analysis. J Hydrol 168:73–89

Pinault JL, Amraoui N, Golaz C (2005) Groundwater induced flooding in macropore-dominated hydrological systems in the context of climate changes. Water Resour Res 41. DOI 10.1029/2004wr0031669-2005

Pinault JL, Plagnes V, Aquelina L, Bakalowicz M (2001) Inverse modeling of the hydrological and hydrochemical behaviour of hydrosystems: characterization of karst system functioning. Water Resour Res 37:2191–2204

Van Camp M, Vauterin P (2005) Tsoft: graphical and interactive software for the analysis of time series and earth tides. Comput Geosci 31:631–640

Wenzel HG (1995) ETERNA package. http://www.eas.slu.edu/GGP/ETERNA. Cited 22 May 2008